Color-Tuning Mechanism in Firefly Luminescence: Theoretical Studies on Fluorescence of Oxyluciferin in Aqueous Solution Using Time Dependent Density Functional Theory

Zhong-wei Li,[†] Ai-min Ren,*[,†] Jing-fu Guo,[‡] Tianxiao Yang,[§] John D. Goddard,[§] and Ji-kang Feng[†]

State Key Laboratory of Theoretical and Computational Chemistry, Institute of Theoretical Chemistry, Jilin University, Changchun 130023, P. R. China, College of Physics, Northeast Normal University, 130024, P. R. China, and Department of Chemistry, University of Guelph, Guelph, Ontario, Canada N1G 2W1

Received: January 24, 2008; Revised Manuscript Received: July 4, 2008

The first singlet excited state geometries of various isomers and tautomers of firefly oxyluciferin ($OxyLH_2$), as well as their fluorescence spectra in aqueous solution, were studied using time dependent density functional theory (TDDFT). With changing pH in aqueous solution, three fluorescence peaks, blue (450 nm), yellow-green (560 nm), and red (620 nm) correspond to neutral keto and enolic forms, the monoanionic enolic form, and the monocationic keto form respectively. A counterion, Na^+, was predicted to cause a blue shift in the fluorescence of anionic $OxyLH_2$. The contributions of a charge transfer (CT) state upon electronic excitation of the planar and twisted structures were predicted. CT was large for the twisted structures but small for the planar ones. The differences between p*K* and p*K** of various oxyluciferin species were predicted using a Forster cycle. A new possible light emitter, namely, the monocation keto form (keto+1), was considered.

1. Introduction

Chemiluminescence of firefly luciferin-AMP (or its analogues) has emission peaks in the red and green with changes in pH suggesting that their multicolor bioluminescence may be explained by the tautomerism of firefly oxyluciferin ($OxyLH_2$) (Figure 1).[1−7] However it was reported that 5,5-dimethyloxyluciferin, an analogue of oxyluciferin which could emit only red light (630 nm) in chemiluminescence according to the tautomerism model as it exists only in the keto form, was found to emit yellow-green light (560 nm) with luciferase.[8] A theoretical explanation of this result involved the nearby protein residues and AMP with the electrostatic effect of the protein causing the keto form to be a higher energy emitter.[9] Furthermore, Nakatsu et al. reported on the basis of X-ray structural analyses of firefly luciferases that green (560 nm) and red light (613 nm) correspond to tight and loose structures of the active sites respectively.[10] Recently, Ando et al. found that red emission components (620 nm peak and 670 nm peak) were insensitive to pH.[11] The tautomerism mechanism may not be necessary to explain the multicolor bioluminescence of firefly luciferases.

However, pH-sensitive luciferases remain important in studies of bioluminescence.[1,12−18] Oxyluciferin was synthesized long ago, and its absorption and fluorescence spectra were measured in various solvents (such as ethanol, DMSO, and water at different pH) to obtain more detailed information on the color modulation.[19−21] IR and NMR showed that $OxyLH_2$ exists as an enolic form in neutral media.[22] The 371 and 425 nm absorption peaks in DMSO correspond to the neutral enolic form and to this species after deprotonation at 6′-H[23] In aqueous solution, these two absorption peaks shift to 370 and 415 nm.[20] The 10 nm blue shift of the anionic enolic form is caused by increasing solvent polarity and is supported by theoretical results.[24,25] On the other hand, fluorescence peaks at 450 and 570 nm in aqueous solution correspond to enol0 and its form with deprotonation at 6′-H. The 620 nm peak was thought to be produced by the keto form.[20] Later the 570 nm peak was separated into 556 nm and 587 nm peaks, which correspond to enol−2 and enol−1.[17] Interestingly, previous theoretical studies did not agree with these results very well. For example, according to SAC-CI (symmetry-adapted cluster-configuration interaction) and CASSCF (complete active space self-consistent field) and TDDFT (time dependent density functional theory), enol−1 always has a lower emission energy than keto−1 and enol−2 has the lowest emission energy.[9,24,26] The details of tautomerism and the fluorescence spectra of oxyluciferin in solvent need to be expounded further prior to considering the even more complicated case of bioluminescence.

Proton transfer (PT) and excited state intramolecular proton transfer (ESIPT) are the keys to understanding tautomerism. Proton transfers can be analyzed in terms of the p*K* and p*K** values of corresponding oxyluciferin species. A Forster cycle is employed here to study the changes in acidity and basicity of $OxyLH_2$ from the ground state (S_0) to the lowest excited state (S_1).[27] Further, we compared the predicted emission spectra with experimental emission spectra to explain the multicolor fluorescence of $OxyLH_2$.

In addition, luciferin-AMP in water with imidazole and in DMSO with potassium *tert*-butoxide produce similar red chemiluminescence ($\lambda_{max} = 650$ nm and $\lambda_{max} = 630$ nm respectively).[2] The emitter was thought to be keto−1, and the blue shift in λ_{max} appeared to be in a progression from more to less polar surroundings.[2,3] However, the predicted shift was to the red with decreasing solvent polarity.[9,24] Therefore, we assessed other factors that can lead to different shifts in the wavelengths such as changes in pH, or the effects of a counterion, Na^+.[20]

Density functional theory (DFT) and TDDFT are employed to predict the ground and excited states of $OxyLH_2$. Previously some properties of $OxyLH_2$ were predicted with similar methods.[25] This article adopts another point of view. Notably,

* Corresponding author. Fax: 0431-88945942. E-mail: aimin.ren@gmail.com.
† Jilin University.
‡ Northeast Normal University.
§ University of Guelph.

10.1021/jp8014047 CCC: $40.75
Published on Web 09/04/2008

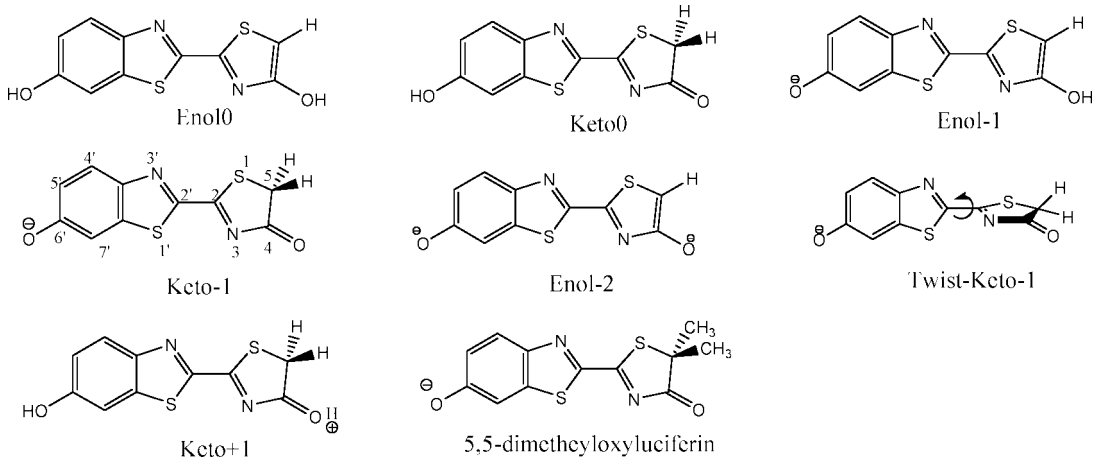

Figure 1. Forms of $OxyLH_2$ and its analogues.

TABLE 1: Predicted Absorption and Emission Spectra, λ_{max}, in nm, and Oscillator Strengths, *f*, Predicted for $OxyLH_2$ in PCM Water with TD B3LYP/6-31+G*

	absorption spectra[a]					emission spectra		
	water/gas[b]		water/water			water/gas		
	λ_{max}	*f*	λ_{max}	*f*	exp[20] λ_{max}	λ_{max}	*f*	exp[20] λ_{max}
enol0	388.08	0.6591	389.33	0.6633	370	453.97	0.6647	450
keto0	411.28	0.4333	419.56	0.4539		458.71	0.2964	
enol−1	488.86	0.7475	478.19	0.6905	415	508.04	0.5957	560
keto−1	507.47	0.7964	512.03	0.7703		559.05	0.5681	
enol−2	498.50	0.5702	495.07	0.5768		572.87	0.4791	
keto+1	517.47	0.3293	517.36	0.3141		605.73	0.0789	620

[a] Absorption spectra predicted by TD B3LYP/6-31+g*//B3LYP/6-31+G*; and emission spectra by TD B3LYP/6-31+G*// TD B3LYP/6-31+G*. [b] Water/gas means an excitation energy calculation in PCM water based on geometry optimization in the gas phase. Similarly, water/water means an excitation energy calculation in PCM water based on geometry optimization in PCM water.

TDDFT has been criticized for its predictions on $OxyLH_2$ due to the possibility of charge transfer (CT) states for which TDDFT with the usual exchange-correlation functionals is known to have difficulties.[26,28,29] Herein, we examine any CT contributions to the excited state before employing TDDFT.

2. Computational Methods

The 6-31+G* basis set, which includes diffuse functions and d-type polarization functions, was employed except for molecules containing sodium, where the 6-31G* set was used instead.

All the ground state geometries were optimized by B3LYP (Becke's hybrid exchange functional and the correlation functional of Lee, Yang, and Parr)[14,30] in Gaussian03.[31] The first excited state geometries of the oxyluciferin molecules were optimized with TD B3LYP in TURBOMOLE.[32]

In order to consider solvent effects on excitation energies, we adopted the polarized continuum model (PCM)[33,34] in Gaussian03 and not the conductor-like screening model (COSMO)[35] which interfaces with Turbomole. Excitation energy predictions were performed with TD B3LYP in Gaussian03. The local correlation function SVWN3 or SVWN5 in B3 depends on whether Gaussian03 or Turbomole was used. SVWN3 is included in B3 Gaussian03 and SVWN5 in B3 in Turbomole. For oxyluciferin molecules, the results with the two functionals were compared (see Figure S3 in Supporting Information).

Before using TDDFT to predict $OxyLH_2$ emission energies, we addressed a possible problem. LH_2 was found to have a charge transfer state as its first excited state.[36] Thus TDDFT may underestimate excitation energies of $OxyLH_2$ due to possible charge transfer contributions[9,26] similar to the case of LH_2. Herein, the natural bond orbital (NBO)[37] analysis in Gaussian03 was used to study their atomic charge assignments. Ground state charges were predicted with B3LYP. For the excited state, NBO could not be used in conjunction with TD B3LYP since TDDFT in Gaussian03 does not produce an excited state density. Another method, configuration interaction with single excitations (CIS) was employed to predict excited state charge distributions. The general features of the flow of the charge distribution are not affected by the use of the CIS method as compared to TDDFT. A TDDFT prediction of the CT state is somewhat contentious although TDDFT may still be effective in geometry optimization.[38] As a specific example, at the TD B3LYP optimized first excited state geometries of keto−1, atomic charge assignments were predicted for the essentially planar structures which are minima in both S_1 and S_0[9,24−26]) and twisted structures (which once were assigned to the red emitter but recently discounted due to the small oscillator strengths of the S_1-S_0 transition[9,26]). The planar form showed a small CT contribution, with only 0.118 negative charges transferred from the benzothiazole moiety to the thiazoline. In contrast 0.708 electron was transferred in twisted keto−1, which was thought to possess a TICT state upon electronic excitation (see Figure S4 in Supporting Information.). The CT contribution in the planar $OxyLH_2$ species is small, and TDDFT should be adequate for predicting the electronic excitations. Further indications of the adequacy of TD B3LYP for the prediction of the emission of keto−1 at 556 nm come from comparison with the previous CASSCF result of 527.6 nm.[26]

When discussing the effects of counterions on the excited state geometries of $OxyLH_2$ Na complexes, the PCM water model must be included. Large charge transfer occurs from $OxyLH_2$ to Na upon excitation in the gas phase (See Figure S5 in Supporting Information.). Thus, in order to employ PCM during excited state geometry optimization, CIS in Gaussian03 was adopted. For emission energy predictions at the optimized CIS geometries TDDFT in Gaussian03 can be used along with PCM.

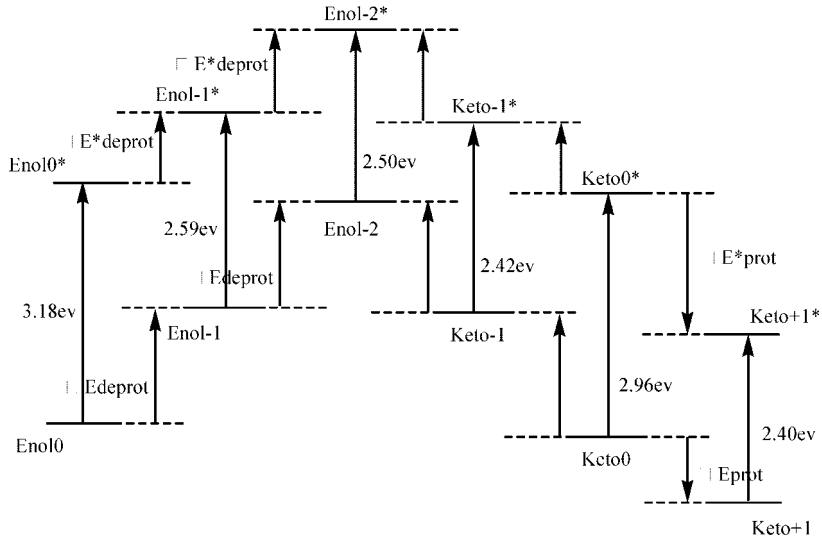

Figure 2. Excitation energies (S_0-S_1) of $OxyLH_2$ predicted by TD B3LYP/6-31+G* //B3LYP/6-31+G* in PCM water. These energies are used in the construction of the Forster cycles discussed in the text.

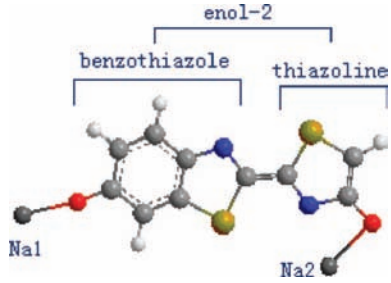

Figure 3. [Enol−2]−2Na complex.

TABLE 2: Emission Spectra, λ_{max}, in nm, and Oscillator Strengths, *f*, Predicted for Anionic $OxyLH_2$ and the Complexes with Na by TD B3LYP/6-31+G*//CIS/6-31G* in PCM Water

	anion		complexes with Na		Na deleted[a]	
	λ_{max}	*f*	λ_{max}	*f*	λ_{max}	*f*
enol−1	506.65	0.8016	499.35	0.7998	506.44	0.8059
keto−1	509.08	0.7798	499.92	0.7680	506.18	0.7866
enol−2	554.83	0.5183	544.17	0.6298	552.44	0.6063

[a] Na deleted: energies calculated at geometries without Na, which were simply deleted from the previously optimized geometries with Na.

TABLE 3: Charge Distribution, in au, in the Benzothiazole and Thiazoline Moieties of Enol−2 and the [Enol−2]−2Na Complex Predicted by CIS/6-31+G*//CIS/6-31G* in PCM Water

	benzothiazole	thiazoline	Na_1	Na_2
enol−2	−0.977	−1.020		
[enol−2]−Na	−0.954	−1.023	0.996	0.981

3. Results and Discussion

3.1. Combining the Present Theoretical and Previous Experimental Results. Now consider the absorption spectra and the steady state fluorescence spectra[20] of $OxyLH_2$ in actual aqueous solutions. The spectra are mainly affected by changes in pH.

The two absorption wavelength maxima, 370 nm in acidic and 415 nm in basic solutions,[20] indicate that there were at least two ground state species, that probably correspond to the neutral form and that deprotonated at 6′-H, namely, enol0 and enol−1 (Table 1). The 4-H in enol−1 is unlikely to be deprotonated for there is no change in the maximum wavelength upon increasing the pH, while the absorption spectrum of enol−2 was predicted to red shift (approximately 15 nm) compared with the monoanions. Comparing the results of water/gas and water/water for oxyluciferin molecules, the PCM solvent model causes only small changes in the spectra after geometry optimization. Thus, for excited state geometry optimization, solvent effects on geometries were not included and computations were of the type water/gas.

In experiments the fluorescence spectra exhibited three wavelength maxima at different pH (pH > 9, 560 nm; 8 > pH > 3, 450 nm; pH < 3, 620 nm).[20] The maximum at 450 nm (blue fluorescence) was produced by enol0 as supported by the TDDFT predictions (Table 1) and the experiments.[20] Only blue fluorescence was observed in ethanol, which inhibited proton transfer, or with $MeOLH_2$ (6′-methoxyluciferin), which has no 6′-H for deprotonation.[20]

With increasing pH, the 6′-H of oxyluciferin doubtlessly ionizes in the ground state and the yellow-green fluorescence corresponds to enol−1. Could such a transformation occur in the excited state of the neutral forms as well? What is more, will the monoanion (enol−1) become a dianion (enol−2) before a radiative transition? The pK_a^* for the 6′-H was thought to decrease upon electronic excitation.[1,2,7,17,20,36] A Forster cycle,[27] which incorporates the acidity and the basicity of various species of $OxyLH_2$, is given in Figure 2 and used to discuss changes from p*K* to p*K**.

Taking enol0 and enol−1 as examples, the Forster cycle is illustrated on the left-hand side of Figure 2. ΔE_{deprot} and ΔE^*_{deprot} are the energies required for deprotonation of enol0 in the ground and the first singlet excited states respectively. The smaller the deprotonation energy, the higher the acidity of either electronic state. With reference to Figure 2 consider the equations

$$\Delta E_{\mathrm{deprot(enol0-enol-1)}} + \Delta E_{\mathrm{enol-1^*-enol-1}} = \Delta E^*_{\mathrm{deprot(enol0^*-enol-1^*)}} + \Delta E_{\mathrm{enol0^*-enol0}} \quad (1)$$

$$\Delta\Delta E_{\mathrm{deprot(enol0)}} = \Delta E_{\mathrm{deprot(enol0-enol-1)}} - \Delta E^*_{\mathrm{deprot(enol0^*-enol-1^*)}} \quad (2)$$

where $\Delta\Delta E_{deprot(enol0)}$ is the acidity change in enol0 upon electronic excitation. Similarly, taking the cycle of keto0 and

keto+1 on the right-hand side of Figure 2 as an example, ΔE_{prot} and ΔE^*_{prot} are the energies released upon protonation of keto0. The more energy that is released, the higher the basicity of keto0. From the figure,

$$\Delta\Delta E_{prot(keto0)} = \Delta E^*_{prot(keto+1^*-keto0^*)} - \Delta E_{prot(keto+1-keto0)} \quad (3)$$

is the basicity change of keto0 upon electronic excitation.

Figure 2 shows the energy values associated with seven different cycles and provides the following information: (1) The acidity of 6′-H in enol0 increases markedly upon electronic excitation in keto0.

$$\begin{aligned} \Delta\Delta E_{deprot(enol0)} &= 3.18\ \text{eV} - 2.59\ \text{eV} \\ &= 0.59\ \text{eV}, \\ \Delta\Delta E_{deprot(keto0)} &= 2.96\ \text{eV} - 2.42\ \text{eV} \\ &= 0.54\ \text{eV} \end{aligned} \quad (4)$$

The ionization of 6′-H could occur in the excited state. (2) If enol−1 or keto−1 do not lose the proton in the ground state, it is impossible for them to transform to enol−2 by deprotonation in the excited state. The values of their $\Delta\Delta E_{deprot}$ are small,

$$\begin{aligned} \Delta\Delta E_{deprot(enol-1)} &= 2.59\ \text{eV} - 2.50\ \text{eV} \\ &= 0.1\ \text{eV}, \\ \Delta\Delta E_{deprot(keto-1)} &= 2.42\ \text{eV} - 2.50\ \text{eV} \\ &= -0.07\ \text{eV} \end{aligned} \quad (5)$$

as enol−1 and keto−1 show less change of acidity upon excitation. (3) Keto+1 could be formed from enol0 or keto0 by protonation in the excited state because the corresponding ΔE^*_{prot} is markedly larger than ΔE_{prot} in the corresponding Forster cycle

$$\begin{aligned} \Delta\Delta E_{prot(keto0)} &= 2.96\ \text{eV} - 2.39\ \text{eV} \\ &= 0.57\ \text{eV}, \\ \Delta\Delta E_{prot(enol0)} &= 3.18\ \text{eV} - 2.39\ \text{eV} \\ &= 0.79\ \text{eV} \end{aligned} \quad (6)$$

The basicity of 5-C in enol0 or of the 4-carbonyl oxygen in keto0 greatly increases upon electronic excitation.

Taking a comprehensive view, it can be deduced that no fluorescence maximum in aqueous solution corresponds to enol−2 as it cannot be formed in either the ground or excited state. The yellow-green fluorescence (λ_{max} = 560 nm) corresponded to enol−1. The observed single exponential fluorescence decay of $OxyLH_2$ in the yellow-green region in aqueous solution (pH = 7.8) supports this conclusion.[20] In addition, at much greater concentration of H^+ (pH < 3), the neutral forms (3 < pH < 8, λ_{max} = 450 nm) could be protonated rather than deprotonated. Keto+1 is a possible red light emitter (λ_{max} = 620 nm). The present theoretical prediction (605.73 nm) agrees very well with the earlier experimental result.

3.2. Effects of Counterions. In order to mimic the experimental environment in the chemiluminescence experiments which were carried out in DMSO with added potassium *tert*-butoxide,[3,4] Nakatani et al. added K^+ ions to the various anionic forms of $OxyLH_2$ in their calculations.[9] The emission spectra shifted to the blue compared to the computations without the potassium ions.[9] To our knowledge, that was the first attempt to consider the counterions in the computational models of oxyluciferin fluorescence. As NaOH was used to alter the pH in aqueous solution in several experiments,[20] the [enol−2]−2Na tight ion pair complex (see Figure 3) was considered to reveal the effects of counterions. The model is somewhat oversimplified as in the real aqueous solution the sodium cations also would interact explicitly with water molecules.

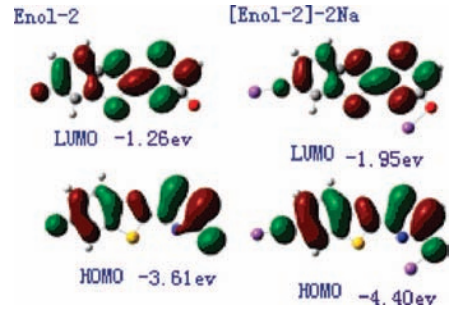

Figure 4. Kohn−Sham frontier orbitals for enol−2 and the [enol−2]−2Na complex predicted with the B3LYP/6-31+G* method in PCM water.

Inclusion of Na^+ causes a 10−20 nm blue shift in the emission spectra, λ_{max}, of the anions. In order to ensure that this effect is due to the Na^+, based on optimized Na complex geometries, Na was deleted from the optimized geometries of the complexes and emission energies were calculated. Virtually no differences are seen (compare the first and third sets of data in Table 2).

How does the Na^+ affect the spectra? Taking enol−2 and its Na complex ([enol−2]−2Na), for example (Figure 3), the charge assignments in the exited state of [enol−2]−2Na are given in Table 3. Na^+ is formed in PCM water. Their Kohn−Sham frontier orbitals, HOMO and LUMO, are shown in Figure 4. Clearly the HOMO and LUMO have very similar characteristics with or without the sodiums, viz., there is no orbital contribution from the Na. Thus, Na^+ affects the emission energies neither by sharing the negative charge of [enol−2] nor by significantly changing the forms of the HOMO and LUMO. However, the sodium does change the KS eigenvalues of enol−2, which leads to a larger energy gap. The $\Delta\varepsilon_{LUMO-HOMO}$ of enol−2 is 2.35 eV; and with Na^+ included the gap is 2.45 eV.

The KS frontier orbital eigenvalues of enol−1, keto−1, and enol−2 are given in Table 4. Na^+ stabilizes the HOMO, and as a result the spectra shift a little to the blue. Accordingly, the blue shift of keto−1 chemiluminescence, which occurs on going from water/imidazole to DMSO/potassium *tert*-butoxide,[2,3] is due to the K^+ counterions in DMSO.

TABLE 4: Kohn−Sham Frontier Orbital Eigenvalues, in eV, Predicted for Anionic $OxyLH_2$ and the Complexes with Na by B3LYP/6-31+G* in PCM Water[a]

	anion			complexes with Na			Na deleted		
	HOMO	LUMO	Δ	HOMO	LUMO	Δ	HOMO	LUMO	Δ
enol−1	−4.65	−2.09	2.56	−4.77	−2.17	2.60	−4.66	−2.10	2.56
keto−1	−5.19	−2.70	2.49	−5.32	−2.77	2.55	−5.18	−2.68	2.50
enol−2	−3.61	−1.26	2.35	−4.40	−1.95	2.45	−4.20	−1.77	2.43

[a] Energy gaps between HOMO and LUMO are reported.

4. Conclusions

In this study, the mechanism for the fluorescence color tuning of firefly oxyluciferin in aqueous solution was expounded with the use of the TDDFT B3LYP/6-31+g* model. From the predicted emission spectra of various isomers and tautomers of oxyluciferin, they are shown to be good emitters in the visible light region. Each species cannot be considered as a fluorescent emitter solely due to agreement between the predicted emission energy and experiment. Keto−1, for example, which was thought to produce the red fluorescence, has no corresponding fluorescence peak in aqueous solution. However, it is still a candidate as the red light emitter in chemiluminescence and bioluminescence for different reaction conditions from those discussed.

In the excited state, neutral $OxyLH_2$ more easily loses its 6′-H proton or gains a proton at 5-C or 4-O. Excited state intramolecular proton transfer may occur. Counterions, such as Na^+ and K^+, cause the emission wavelength of anionic $OxyLH_2$ to shift a little to the blue.

Charge transfer within $OxyLH_2$ is insignificant in the planar forms, and the efficient TDDFT approach proved powerful in studying the series of oxyluciferin molecules.

This report has focused on fluorescence in aqueous solution, which must be differentiated from chemi- or bioluminescence.

Acknowledgment. This work was supported by the National Natural Science Foundation of China (No.20673045) and by the Natural Sciences and Engineering Research Council of Canada.

Supporting Information Available: Full reference for ref 31.The bond lengths and atomic charge assignments for the molecules referred to in this article. This material is available free of charge via the Internet at http://pubs.acs.org.

References and Notes

(1) Vlasova, T. N.; Leontieva, O. V.; Ugarova, N. N. *Biolumin. Chemilumin.: Prog. Perspect.* **2005**, 69–72.
(2) White, E. H.; Rapaport, E.; Seliger, H. H.; Hopkins, T. A. *Bioorg. Chem.* **1971**, *1*, 92.
(3) Hopkins, T. A.; Seliger, H. H.; White, E. H. *J. Am. Chem. Soc.* **1967**, *89*, 7148.
(4) White, E. H.; Rapaport, E.; Hopkins, T. A.; Seliger, H. H. *J. Am. Chem. Soc.* **1969**, *91*, 2178.
(5) White, E. H.; Steinmetz, M. G.; Miano, J. D.; Wildes, P. D.; Morland, R. *J. Am. Chem. Soc.* **1980**, *102*, 3199.
(6) Rhodes, W. C.; McElroy, W. D. *J. Biol. Chem.* **1958**, *233*, 1528.
(7) Leontieva, O. V.; Vlasova, T. N.; Ugarova, N. N. *Biochemistry (Moscow)* **2006**, *71*, 51.
(8) Branchini, B. R.; Murtiashaw, M. H.; Magyar, R. A.; Portier, N. C.; Ruggiero, M. C.; Stroh, J. G. *J. Am. Chem. Soc.* **2002**, *124*, 2112.
(9) Nakatani, N.; Hasegawa, J.; Nakatsuji, H. *J. Am. Chem. Soc.* **2007**, *129*, 8756.
(10) Nakatsu, T.; Ichiyama, S.; Hiratake, J.; Saldanha, A.; Kobashi, N.; Sakata, K.; Kato, H. *Nature* **2006**, *440*, 7082.
(11) Ando, Y.; Niwa, K.; Yamada, K.; Enomoto, T.; Irie, T.; Kubota, H.; Ohmiya, Y.; Akiyama, H. *Nat. Photonics* **2008**, *2*, 44.
(12) Viviani, V. R. *Cell. Mol. Life. Sci.* **2002**, *59*, 1833.
(13) Branchini, B. R.; Magyar, R. A.; Murtiashaw, M. H.; Anderson, S. M.; Helgerson, L. C.; Zimmer, M. *Biochemistry* **1999**, *38*, 13223.
(14) Viviani, V. R.; Oehlmeyer, T. L.; Arnoldi, F. G. C.; Brochetto-Braga, M. R. *Photochem. Photobiol.* **2005**, *81*, 843.
(15) Kitayamay, A.; Yoshizaki1, H.; Ohmiya, Y.; Uedaz, H.; Nagamune, T. *Photochem. Photobiol.* **2003**, *77* (3), 333.
(16) Viviani, V.; Uchida, A.; Suenaga, N.; Ryufuku, M.; Ohmiya, Y. *Biochem. Biophys. Res. Commun.* **2001**, *280*, 1286.
(17) Ugarova, N. N.; Maloshenok, L. G.; Uporov, I. V. *Biochemistry (Moscow)* **2005**, *70*, 1262.
(18) Viviani, V. R.; Arnoldi, F. G. C.; Neto, A. J. S.; Oehlmeyer, T. L.; Bechara, E. J. H.; Ohmiya, Y. *Photochem. Photobiol. Sci.* **2008**, *2*, 159.
(19) Morton, R. A.; Hopkins, T. A.; Seliger, H. H. *Biochemistry* **1969**, *8*, 1598.
(20) Gandelmann; O, A.; Brovko, L.Yu.; Ugarova, N. N.; Chikishevb, A.Yu.; Shkurimov, A. P. *J. Photochem. Photobiol: B* **1993**, *19*, 187.
(21) Wada, N.; Shibata, R. *J. Phys. Soc. Jpn.* **1997**, *66*, 3312.
(22) Suzuki, H.; Goto, T. *Agric. Biol. Chem.* **1972**, *36*, 2213.
(23) Suzuki, N.; Sato, M.; Okada, R.; Goto, T. *Tetrahedron* **1972**, *28*, 4065.
(24) Ren, A. M.; Goddard, J. D. *J. Photochem. Photobiol: B* **2005**, *81*, 163.
(25) Ren, A.-M.; Guo, J.-F.; Feng, J.-K.; Zou, L.-Y.; Li, Z.-W.; Goddard, J. D. *Chin. J. Chem.* **2008**, *26*, 55.
(26) Yang, T.; Goddard, J. D. *J. Phys. Chem. A* **2007**, *111*, 4489.
(27) Catalan, J. *J. Am. Chem. Soc.* **2001**, *123*, 11940.
(28) Fujimoto, K.; Hayashi, S.; Hasegawa, J.; Nakatsuji, H. *J. Chem. Theory Comput.* **2007**, *3*, 605.
(29) Wanko, M.; Hoffmann, M.; Strodel, P.; Koslowski, A.; Thiel, W.; Neese, F.; Frauenheim, T.; Elstner, M. *J. Phys. Chem. B* **2005**, *109*, 3606.
(30) Becke, A. D. *J. Chem. Phys.* **1993**, *98*, 5648.
(31) Frisch, M. J.; et al. *GAUSSIAN 03*, revision A.1; Gaussian, Inc.: Pittsburgh, PA, 2003. Full reference given in Supporting Information.
(32) Ahlrichs, R.; Bar, M. H.; Baron, P.; Bauernschmitt, R.; Bocker, S.; Deglmann, P.; Ehrig, M.; Eichkorn, K.; Elliott, S.; Furche, F.; Haase, F.; Haser, M.; Horn, H.; Hattig, C.; Huber, C.; Huniar, U.; Kattannek, M.; Kohn, A.; Kolmel, C.; Kollwitz, M.; May, K.; Ochsenfeld, C.; Ohm, H.; Patzelt, H.; Rubner, O.; Schafer, A.; Schneider, U.; Sierka, M.; Treutler, O.; Unterreiner, B.; Arnim, M. V.; Weigend, F.; Weis, P.; Weiss, H. *TURBOMOLE-V5-7-patches*; University of Karlsruhe: Karlsruhe, 2004.
(33) Mineva, T.; Russo, N. *Int. J. Quantum Chem.* **1997**, *61*, 665.
(34) Houjou, H.; Inoue, Y.; Sakurai, M. *J. Am. Chem. Soc.* **1998**, *120*, 4459.
(35) Eckert, F.; Klant, A. *AIChE J.* **2002**, *48*, 369.
(36) Jung, J.; Chin, C. A.; Song, P. S. *J. Am. Chem. Soc.* **1976**, *98*, 3949.
(37) (a) NBO Version 3.1: Glendening, E. D.; Reed, A. E.; Carpenter, J. E.; Weinhold, F. (b) Carpenter, J. E.; Weinhold, F. *J. Mol. Struct. (Theochem).* **1988**, *169*, 41. (c) Carpenter, J. E. PhD Thesis, University of Wisconsin, Madison, WI, 1987. (d) Foster, J. P.; Weinhold, F. *J. Am. Chem. Soc.* **1980**, *102*, 7211. (e) Reed, A. E.; Weinhold, F. *J. Chem. Phys.* **1983**, *78*, 4066. (f) Reed, A. E.; Weinstock, R. B.; Weinhold, F. *J. Chem. Phys.* **1985**, *83*, 735. (g) Reed, A. E.; Curtiss, L. A.; Weinhold, F. *Chem. Rev.* **1988**, *88*, 899.
(38) Van Caillie, C.; Amos, R. D. *Chem. Phys. Lett.* **2000**, *317*, 159.

JP8014047